Front. Electr. Electron. Eng. China 2009, 4(3): 335–341
DOI 10.1007/s11460-009-0033-y

RESEARCH ARTICLE

A. GOURBI, M. BRAHAMI, A. TILMATINE, P. PIROTTE

Numerical simulation of corona-induced vibration of high voltage conductor

Abstract When it rains, electric power transmission lines start vibrating due to corona effect. This type of vibration is known as "corona-induced vibration". The aim of this paper is to elaborate a mathematical model for numerical simulation of the corona-induced vibration, with consideration of the influence of the magnitude and the polarity of the electric field on the conductor surface. Finite element method was employed to develop the numerical model, and the finite difference method was used for the time discretisation. The moment of application of the corona-induced force is evaluated using the resultant vertical force applied to a water drop, suspended under a high voltage conductor. Some experimental results of other authors are exploited to evaluate the precision of the simulation and the validation of numerical results.

Keywords corona-induced vibration, corona wind, finite element method

1 Introduction

One of the consequences of high voltage electric power systems is the corona effect. This phenomenon is the source of electromagnetic interference, audible noises, important energy losses and mechanical vibrations. This latter consequence, called "corona-induced vibration", can lead to the fatigue of overhead conductors and supporting elements [1]. It has been established that the intermittent presence of corona space charge and the ionic wind are the main causes of this phenomenon. Research in this field began in 1970 by an analytical study focusing on the determination of vibration amplitudes. Following studies, this time with experimental detail, realized in Canada, led to a significant result and especially interest in the mechanism of vibrations [2,3]. Then, in 1986 a precise mechanism was proposed and accepted by the scientific community [4]. During these years many researchers have studied the different aspects of this subject. Diverse experimental models and laboratory mechanisms were used to simulate this phenomenon. However, most of the researchers accomplished the successive results but few of these results were based on a numerical model and numerical simulation. Therefore, the present work is based on the numerical simulations of the corona-induced vibration [5]. Two simulation techniques are used: the modal superposition for the discretisation of the movement, and the central difference method for the discretisation of the time. Some experimental results of other authors are exploited to evaluate the accuracy of the numerical simulation.

Received June 12, 2008; accepted October 14, 2008

A. GOURBI (✉), M. BRAHAMI, A. TILMATINE, P. PIROTTE
Djillali Liabes University, Sidi Bel Abbés 22000, Algeria
E-mail: aekett@yahoo.fr

2 Description of vibration mechanism

The vibration mechanism can be described by the following steps (Fig. 1) [6–11]:

1) The conductor is attracted to the ground surface, due to the electric image force.

2) Under wet conditions and in the presence of electric field, suspended drops are formed at the lower surface of the conductor.

3) The suspended drops at the bottom of the conductor surface take on a conical shape. The formation of cones results from the interaction between the forces due to the electrostatic field on the surface of the conductor, surface tension and gravity.

4) Due to the field intensification at the tip of the cones, corona discharge increases the space charge around the suspended water drops.

5) The increase of the space charge around water drops produces a partial shielding effect between the conductor and the ground.

6) The electric image force is eliminated and thus the conductor moves upward.

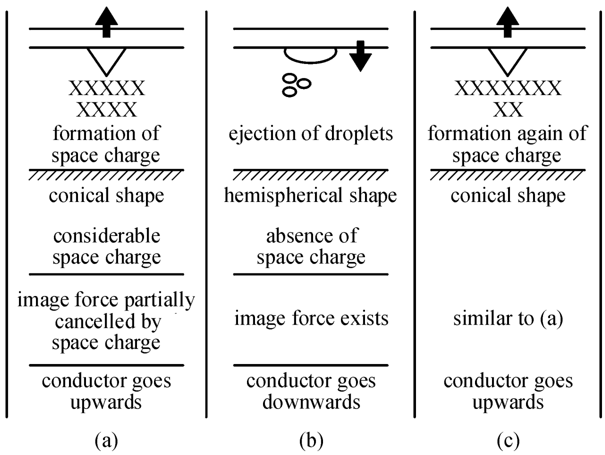

Fig. 1 Corona-induced vibration mechanism

7) The suspended drops reach a critical size, instability occurs and a certain quantity of the water drop is ejected from the conductor.

8) Corona discharge is attenuated and therefore the current decreases to a small value. The water drops remaining on the conductor surface do not have the conical shape, consequently the corona discharge is very weak and the space charge becomes small.

9) Therefore, there is no shielding produced by the space charge and thus the attractive force between the conductor and the ground becomes important again; the conductor moves downward.

10) As the rain continues, more water flows, and the conical shape of the drops produces again the space charge, thus the process is repeated (continuous vibration).

3 Development of basic differential equation

We first determine the basic differential equation that describes the tense-conductor vertical displacements submitted to a distributed external force.

First, let us consider the governing differential equations of the suspended cable:

$$\rho(x)\frac{\partial^2 U(x,t)}{\partial t^2}+\mu(x)\frac{\partial U(x,t)}{\partial t}-\frac{\partial}{\partial x}\left[\alpha(x)\frac{\partial U(x,t)}{\partial x}\right]=f(x,t), \tag{1}$$

where $\rho(x)\dfrac{\partial^2 U(x,t)}{\partial t^2}$ is inertia force term, $\mu(x)\dfrac{\partial U(x,t)}{\partial t}$ is damping force term, $\dfrac{\partial}{\partial x}\left[\alpha(x)\dfrac{\partial U(x,t)}{\partial x}\right]$ is conductor tension force term, $f(x,t)$ is external forces, $U(x,t)$ is vertical conductor displacement.

Equation (1) is solved using the finite element method; this method is a numerical analysis technique for obtaining approximate solutions to a wide variety of engineering problems. The GALERKIN technique leads to the decrease in the integration order [12,13].

The typical pondered residual equation can be written as follows:

$$\int^{e} R(x,t;a)\Phi_i(x)\mathrm{d}x=0, \tag{2}$$

where

$$R(x,t;a)=\rho(x)\frac{\partial^2 U(x,t)}{\partial t^2}+\mu(x)\frac{\partial U(x,t)}{\partial t}-\frac{\partial}{\partial x}\left[\alpha(x)\frac{\partial U(x,t)}{\partial x}\right]-f(x,t),$$

and $\Phi_i(x)$ is a polynomial interpolation function.

When developing the integral part, we obtain

$$\int^{e}\Phi_i^e(x)\rho(x)\frac{\partial^2\tilde{U}^e(x,t)}{\partial t^2}\mathrm{d}x+\int^{e}\Phi_i^e(x)\mu(x)\frac{\partial\tilde{U}^e(x,t)}{\partial t}\mathrm{d}x+\int^{e}\frac{\mathrm{d}\Phi_i^e(x)}{\mathrm{d}x}\alpha(x)\frac{\partial\tilde{U}^e(x,t)}{\partial x}\mathrm{d}x=\int^{e}f(x,t)\Phi_i^e(x)\mathrm{d}x-\left[\left(-\alpha(x)\frac{\partial\tilde{U}^e(x,t)}{\partial x}\right)\Phi_i^e(x)\right]_{x_1}^{x_n}. \tag{3}$$

We adopt now an approximate solution to the problem:

$$\tilde{U}^e(x,t;a)=\sum_{j=1}^{n}a_j(t)\Phi_j^e(x), \tag{4}$$

where $a_j(t)$ represents the values of the function $\tilde{U}$ at the different nodes, and n is the liberty degrees.

When substituting the approximate solution and its derivative:

$$\frac{\partial\tilde{U}^e(x,t)}{\partial x}=\sum_{j=1}^{n}a_j(t)\frac{\mathrm{d}\Phi_j(x)}{\mathrm{d}x},$$

$$\frac{\partial\tilde{U}^e(x,t)}{\partial t}=\sum_{j=1}^{n}\frac{\mathrm{d}a_j(t)}{\mathrm{d}t}\Phi_j(x),$$

$$\frac{\partial^2\tilde{U}^e(x,t)}{\partial t^2}=\sum_{j=1}^{n}\frac{\mathrm{d}^2a_j(t)}{\mathrm{d}t^2}\Phi_j(x)$$

into Eq. (3), we obtain:

$$M^e\frac{\mathrm{d}^2a(t)}{\mathrm{d}t^2}+C^e\frac{\mathrm{d}a(t)}{\mathrm{d}t}+K^e a(t)=F^e(t), \tag{5}$$

where

$$M_{ij}^e=\int^{e}\Phi_i^e(x)\rho(x)\Phi_j^e(x)\mathrm{d}x,$$